CARMA Large Area Star formation Survey: First Look at Barnard 1

Shaye Storm (UMd), Lee Mundy (UMd), Peter Teuben (UMd), Hector Arce (Yale), Che-Yu Chen (UMd), Richard Crutcher (UIUC), Manuel Fernandez Lopez (UIUC), Charles Gammie (UIUC), Hao Gong (UMd), Nicholas Hakobian (UIUC), Andrea Isella (lower CIT), Jens Kauffmann (JPL), Woojin Kwon (U. Groningen), Katherine Lee (UIUC), Leslie Looney (UIUC), Eve Ostriker (Princeton), Adele Plunkett (Yale), Marc Pound (UMd), Erik Rosolowsky (UBC), Demerese Salter (UMd), Yancy Shirley (UA), Konstantinos Tassis (U. Crete), Leonardo Testi (ESO), John Tobin (NRAO), Nikolaus Volgenau (OVRO/CIT)

BACKGROUND

We present spectral line images of the Perseus Barnard 1 (B1) region. This work is part of the CARMA Large Area Star-formation Survey (CLASSy) Key Project, which is mapping 5 fields in the Perseus and Serpens Molecular Clouds. The main goals of CLASSy are to test the predictions of turbulence-driven star formation, to clarify the relationship between the dense gas and young stellar content of clouds, and to study core evolution. B1 is located 3.5 pc to the east of NGC 1333, and is thought to be in an earlier stage of evolution. The B1 "main core" contains several continuum clumps of cool dust, outflows, and shock activity [2,7,8,9,11,15]. It has been suggested that the main core is in the early stages of collapse and some mechanism, such as magnetic support [3,5,11], is slowing its evolution. This is based on: A) a low stellar-to-gas content ratio for a region with associated optical stars [11], B) higher turbulence decay energy relative to energy input from existing protostellar outflows [7,15], C) the detection of a relatively strong, -27 uG, magnetic field along the line-of-sight [5] and organized grain alignment [11]. The gas and dust southwest of the main core is even less active, providing the opportunity to study star formation along a gradient of evolutionary stages within one region of Perseus. Our observations presented here will enable further development of the story of B1 and nearby, clustered, low-mass star formation.

OBSERVATIONS

- CARMA D and E array
- 23-dish and single-dish observing *(fully imaging molecular lines)*
- 743-pt mosaic covering 150 sq. arcmin.
- 150 total hours
- Synthesized beam ~6.5" x 7.5"
- HCN, HCO^+, N_2H^+ J=1-0
  - 8 MHz bands; ~0.16 km/s resolution
  - Sensitivity per channel ~ 100 mJy/bm
- 3 mm continuum
  - Sensitivity ~ 1.5 mJy/bm

TAKE AWAY POINTS

- We have produced the first large-area (150 sq. arcminute), high-angular resolution (7") spectral line images of B1 in N_2H^+, HCN, and HCO^+ J=1-0 using CARMA.
- Dense, cool gas is present across the entire field. N_2H^+ has the strongest gas-to-dust correspondence, particularly in the main core, while HCO^+ and HCN appear more diffuse and trace the outflows in the main core.
- We see little correspondence between the dense gas peak locations and the locations of existing protostars, except for the Class 0 source, B1-c.
- Two dense, 3 mm continuum cores are detected. We detect the rotating envelope and outflow of B1-c, and find good evidence that the B1-b double core is at an earlier stage of evolution.
- We detect a dynamically coherent, high density, 0.03 x 0.2 pc filament in all three molecules along the edge of the major dust filament. It is possible that we are detecting swept us gas that might fragment into cores in the future.

Large-Scale, High-Resolution View of Dense Gas in B1

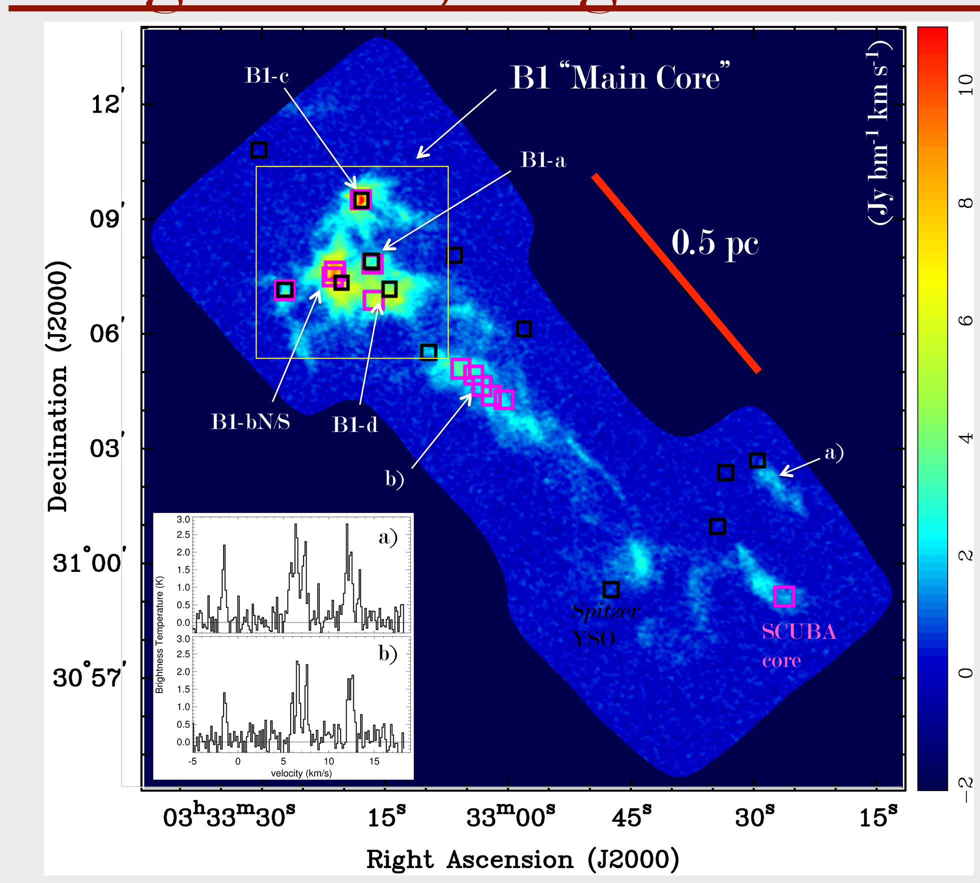

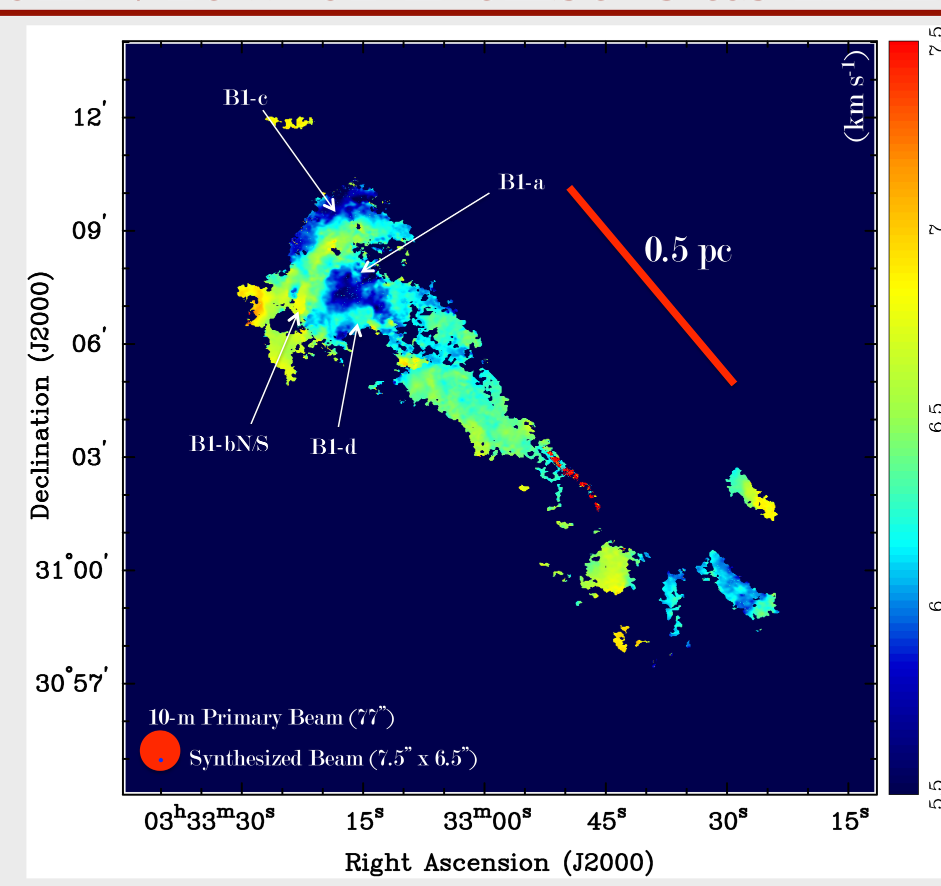

N_2H^+ (1-0) Integrated Intensity and Centroid Velocity Maps: The left image is a zeroth moment map illustrating the distribution of N_2H^+ gas throughout B1. Example spectra sampled within a synthesized beam at two areas of moderate emission are shown in the inset; the sensitivity is ~0.3 K per 0.16 km/s channel. Spitzer YSOs [9] and SCUBA cores [6,10] are identified by black and pink boxes, respectively. The right image shows the best-fit centroid velocities across the field.

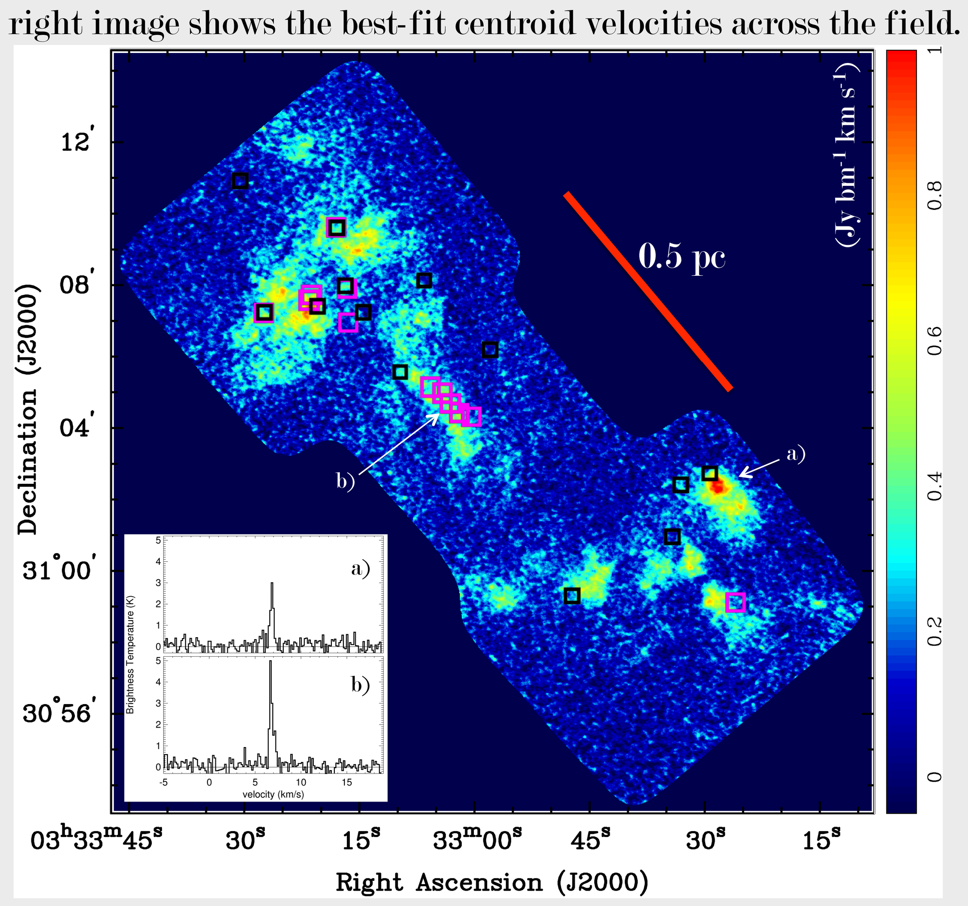

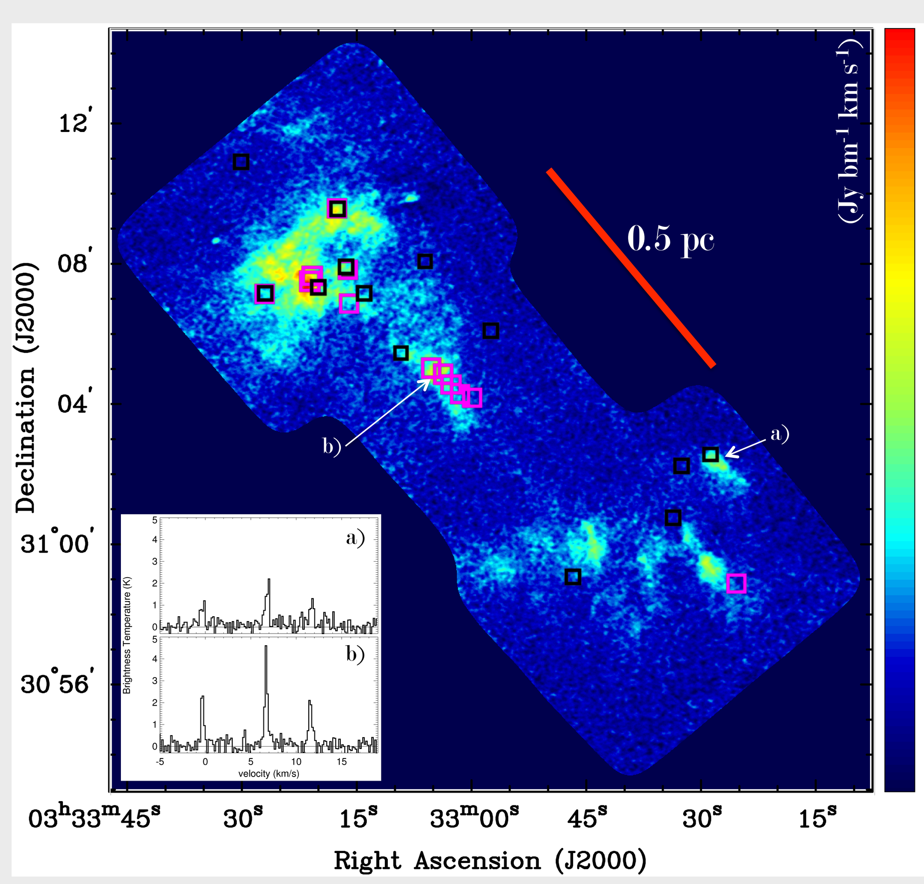

HCO^+ (1-0) and HCN (1-0) Integrated Intensity Maps: The HCO^+ (left) and HCN (right) zeroth moment maps illustrate the distribution of the dense, carbon-bearing, gas; we exclude outflow channels here. There is a strong correlation between the emission seen in these two molecules, except towards evolved dense cores, such as B1-c, where HCO^+ is more strongly depleted.

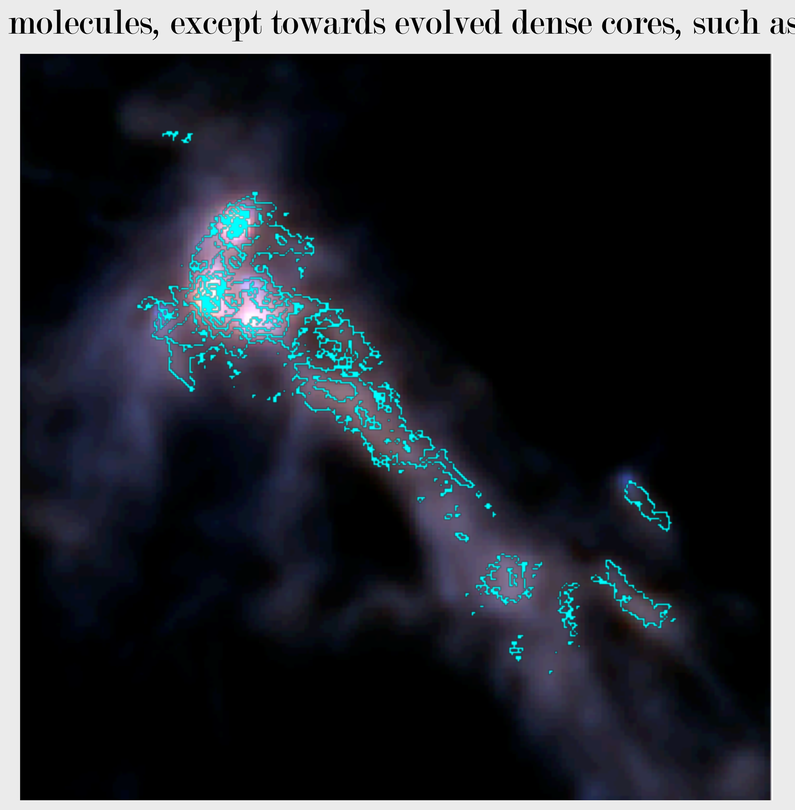

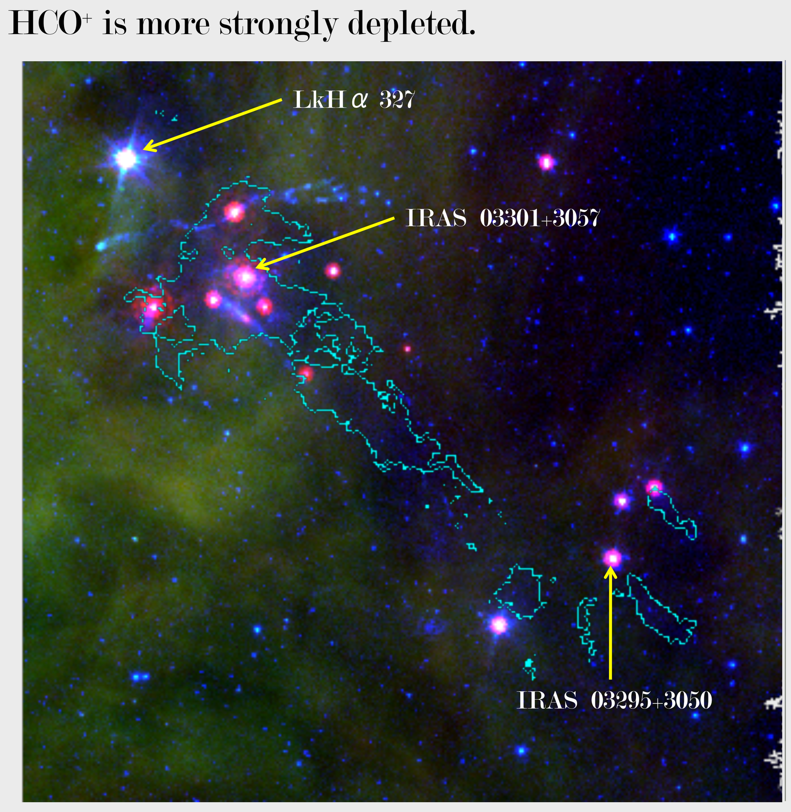

Comparison to *Herschel* and *Spitzer*: The left image shows the *Herschel* SPIRE [1] view of B1 with our N_2H^+ contours overlaid. There is a nonlinear correspondence between the cool dust and the dense gas; the two are in closest agreement in the main core, where more dense cores have started to form compared to the southwest filament and clumps. The right image shows the *Spitzer* view [9] of B1 with a low-emission N_2H^+ contour. IRAC2 is a good tracers of outflows, which we detect in HCN and HCO^+ (see "Main Core" section); IRAC 4 and MIPS 1 highlight the red protostars. There does not appear to be a strong correlation between existing protostars and the locations of dense gas peaks (except for B1-c).

Structure and Kinematics of B1 Main Core

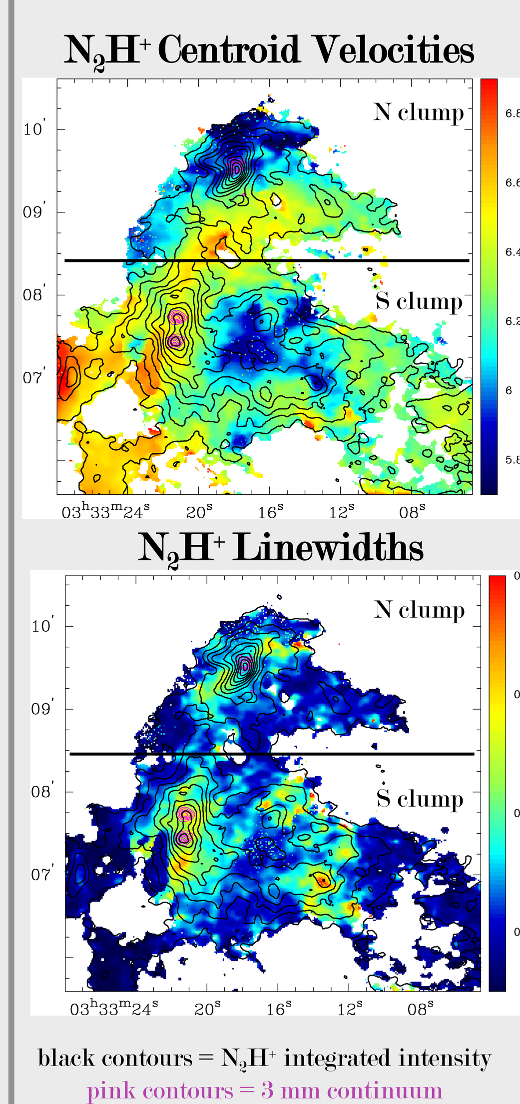

B1 Main Core: These maps capture the kinematics and structure of the cool, dense gas in the main core. The gas can be divided into a northern and southern clump (similar to previous low-resolution NH_3 observations [2]); both clumps have a large scale centroid velocity gradient of ~6 km s^{-1} pc^{-1} at their maximum, though the direction of the gradient between the two clumps is nearly orthogonal. 3 mm continuum emission is plotted with pink contours, and only the B1-c and B1-b continuum cores are identified. The linewidth map shows the impact of the B1-c outflow in the northern clump. In the southern clump, there is a lot of variation in linewidth, with a plateau of increased linewidth around the B1-b core.

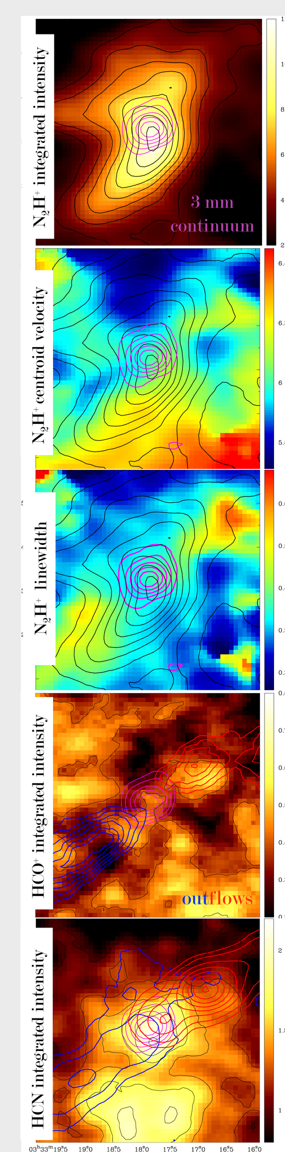

B1-c: This dense core has been classified as a Class 0 protostar based on its rotating N_2H^+ envelope, strong HCO^+ outflow, anti-correlation of N_2H^+ with HCO^+ at the source position, depletion of N_2H^+ towards the continuum center [12], and associated *Spitzer* YSO [9]. We recover the gas features nicely in our maps (though we lack the resolution to detect the central N_2H^+ depletion), giving us confidence in our results on small spatial scales. Our large-scale view of the main B1 core allows us to see that the rotation pattern of the B1-c N_2H^+ envelope extends across the northern clump of the main core. The increased N_2H^+ linewidth axis follows the HCN and HCO^+ outflow axes.

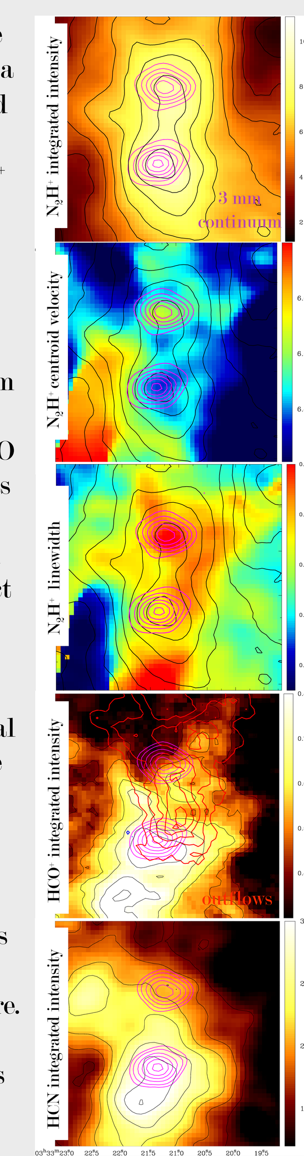

B1-b: This double core system is not associated with any infrared source, is thought to be younger than a typical Class 0 protostar and is a possible FHSC candidate [8]. We observe two resolved peaks of continuum and N_2H^+ emission. The N_2H^+ centroid velocities show possible E-W rotation in the southern core. The N_2H^+ linewidths show the cores forming in a region of increased turbulence. Although theory and observations predict that cores fragment in regions of coherent, subsonic gas [e.g., 4, 14], B1-b has likely evolved to disrupt its natal state. It is possible that the N_2H^+ gas is being stirred by the weakly-collimated HCO^+ outflow that we detect, which may be originating from the southern source (no blue wing is detected). The weak HCO^+ outflow and lack of HCN outflow are indications that B1-b has not evolved to a Class 0 stage, while the HCO^+ outflow is still consistent with recent MHD simulations showing that FHSCs can drive molecular outflows [17].

Narrow Gas Filament Along Edge of Larger Dust Filament

Observed Molecular Properties

- Seen in all 3 molecules
- Width ~ 20"; ~ 0.025 pc [5000 AU] at 250 pc
- Length ~ 2.5'; ~ 0.2 pc [41,000 AU] at 250 pc
- Spectral features along filament
  - +1.5 km/s redshifted from bulk gas

  Average line width:
  - N_2H^+ σ_{obs} ~ 0.12 km/s
  - HCN σ_{obs} ~ 0.17 km/s
  - HCO^+ σ_{obs} ~ 0.20 km/s

  Average peak brightness temperature:
  - N_2H^+ ~ 2.9 K
  - HCN ~ 2.9 K
  - HCO^+ ~ 3.7 K
- 10 K gas temperature [16]
  - Even with a high column density, need $n \geq 10^5$ cm^{-3} to get observed temperatures, in agreement with n_{cr} for these molecules.
  - N_2H^+ and HCN exhibit subsonic nonthermal linewidths at this temperature; HCO^+ linewidths are sonic.

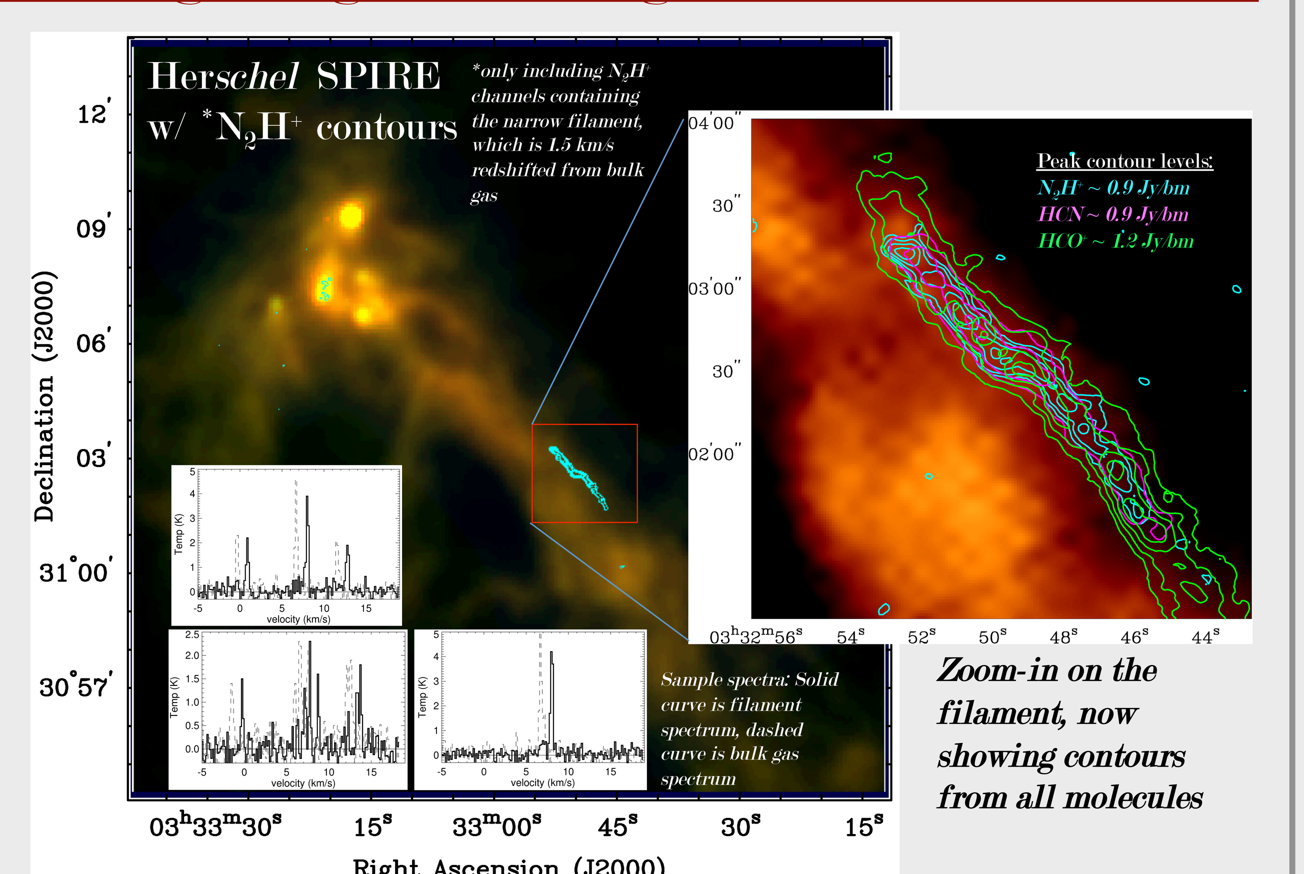

Zoom-in on the filament, now showing contours from all molecules

Explanations: Swept up gas? Self-gravitating cylinder?

The 1.5 km/s radial velocity of the gas filament relative to the bulk B1 gas suggests that it did not fragment from the main reservoir of B1 gas.

- Perhaps a flow from in front of the *Herschel* filament (green arrows), with some positive velocity component along our line of sight, caused a pileup of material. Some of this material may have flowed around the western edge of the *Herschel* filament, causing the density to increase along the edge, thereby strengthening the molecular emission from dense gas tracers and causing the redshift.
- However, we would expect such a dynamic event to produce more turbulent linewidths across the filament.
- Perhaps this impact happened long enough ago for gravity to collect the gas into a filament.
  - We fit the radial integrated intensity profile with a cylindrical filament model for each molecule. Each case fits better with $p=4$ (isothermal structure in hydrostatic equilibrium) than shallower profiles.
  - If it is a self-gravitating, isothermal cylinder, there would be ~ 1 $M_\odot$ along its length available to fragment into dense cores [13].
  - With a Jean's Length ~10,000 AU for T=10 K, n ~ 10^5 cm^{-3} gas, this 41,000 AU filament could fragment to form cores in the future.

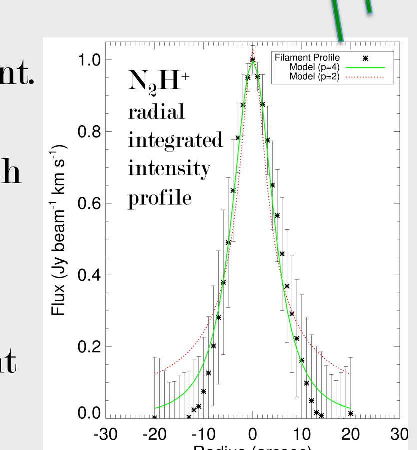

Grants: CARMA is supported through the NSF URO program. CLASSy work was supported by AST 1139990, 1139950, 1140063.

References: [1] Andre et al. 2011 EAS 52 167 • [2] Bachiller et al. 1990 A&A 236 461 • [3] Crutcher et al. 1994 ApJ 427 839 • [4] Gong & Ostriker 2011 ApJ 729 120 • [5] Goodman et al. 1989 ApJL 338 61 • [6] Hatchell et al. 2005 A&A 440 151 • [7] Hiramatsu et al. 2010 ApJ 712 778 • [8] Hirano et al. 1999 Star Formation 1999 181 • [9] Jorgensen et al. 2006 ApJ 645 1246 • [10] Kirk et al. 2006 ApJ 646 1009 • [11] Matthews et al. 2002 ApJ 574 822 • [12] Matthews et al. 2006 ApJ 652 1374 • [13] Ostriker J. 1964 ApJ 140 1056 • [14] Pineda et al. 2011 ApJL 739 2 • [15] Walawender et al. 2005 ApJ 130 1795 • [16] http://www.cfa.harvard.edu/COMPLETE/ • [17] Machida et al. 2008 ApJ 676 1088